Inorganic Chemistry

Article

pubs.acs.org/IC

Double Sandwich Polyoxometalate and Its Fe(III) Substituted Derivative, $[As_2Fe_5Mo_{21}O_{82}]^{17-}$ and $[As_2Fe_6Mo_{20}O_{80}(H_2O)_2]^{16-}$

Xiangqian Dong, Yanping Zhang, Bin Liu, Yanzhong Zhen, Huaiming Hu, and Ganglin Xue*

Key Laboratory of Synthetic and Natural Functional Molecule Chemistry (Ministry of Education), Department of Chemistry, Northwest University, Xian, 710069, China

Supporting Information

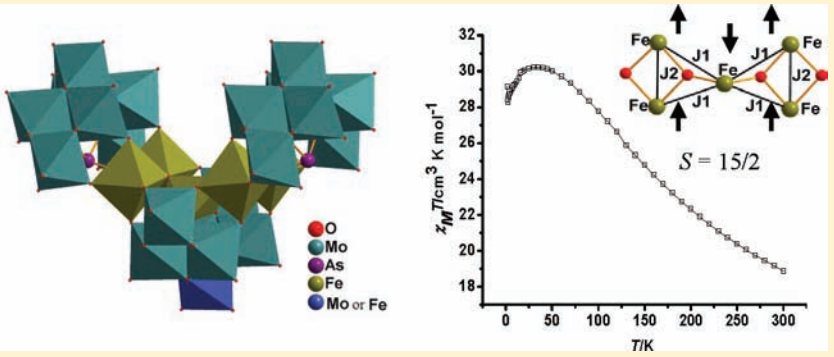

ABSTRACT: A double sandwich polyoxometalate and its Fe(III) substituted derivative, $[As_2Fe_5Mo_{21}O_{82}]^{17-}$ (**1**) and $[As_2Fe_6Mo_{20}O_{80}(H_2O)_2]^{16-}$ (**2**), were synthesized and characterized by single-crystal X-ray diffraction, infrared spectroscopy, fluorescent spectroscopy, UV spectra, thermogravimetry-differential scanning calorimetry analyses, electrospray ionization mass spectrometry, and magnetism measurements. The polyoxoanion is composed of a central fragment $FeMo_7O_{28}$ for **1** ($Fe_2Mo_6O_{26}(H_2O)_2$ for **2**) and two external $AsMo_7O_{27}$ fragments linked together by two distinct edge-sharing dimeric clusters Fe_2O_{10} to lead to a C_{2v} molecular symmetry. The central $FeMo_7O_{28}$ fragment and external $AsMo_7O_{27}$ fragment have a similar structure, and both of them can be viewed as a monocapped hexavacant α-Keggin subunit with a central FeO_4 group or a central AsO_3 group. Both of the polyoxoanions contain a oxo-bridged Fe^{III}_5 magnetic core with the angles of Fe−O−Fe in the range of 96.4(4)−125.7(5)°, and magnetism measurements show an overall ferromagnetic interactions among the five-nuclearity cluster Fe_5 with the spin ground state S = 15/2.

INTRODUCTION

Polyoxometalates (POMs) are a class of discrete metal−oxygen anionic clusters, which exhibit compositional diversity and structural versatility, resulting in potential applications in catalysis, magnetochemistry, medicine, and materials science.[1] POMs are usually composed of early transition metal MO_6 (M = W^{6+}, Mo^{6+}, etc.) octahedra and main group XO_4 (X = P, Si, etc.) tetrahedra. The most famous POMs are probably the Keggin (e.g., $PMo_{12}O_{40}^{3-}$) and the Wells−Dawson (e.g., $P_2W_{18}O_{62}^{6-}$) ions. Nevertheless, also lone-pair-containing main group elements (e.g., As^{3+}, Sb^{3+}, and Bi^{3+}) can act as hetero groups. The important structural feature of POMs containing the subvalent main group atoms is that they can not form the closed Keggin unit. For polyoxotungstates, the trivacant Keggin anion α-$XW_9O_{33}^{9-}$ (X = As^{3+}, Sb^{3+}, and Bi^{3+}) is main species in weakly alkaline or neutral aqueous solution, whereas β-$XW_9O_{33}^{9-}$ anion is main species in weakly acidic aqueous solution, both of them can be used as basic building blocks to form large polyanions, linked by extra W, rare earth ions, organometallic entities, or transition-metal clusters that continue to attract a great deal of interest in several areas of research because of their fascinating chemical and physical properties.[2] Such as dimeric sandwich-type heteropolyanions, $[(M((H_2O))_3(\alpha\text{-}XW_9O_{33})_2]^{n-}$, $[(WO_2)_2M_2(H_2O)_6(\beta\text{-}XW_9O_{33})_2]^{14-}$, $[M_4(H_2O)_{10}(\beta\text{-}XW_9O_{33})_2]^{n-}$, (X = As^{3+}, Sb^{3+}, Bi^{3+}, M = first-row transition metal ion),[3] and $[(C_6H_5Sn)_2As_2W_{19}O_{67}(H_2O)]^{8-}$,[4] trimeric polyanion, $[\{Y(\alpha\text{-}SbW_9O_{31}(OH)_2)\text{-}(CH_3COO)(H_2O)\}_3(WO_4)]^{17-}$,[5] and $[(BiW_9O_{33})_3Bi_6(OH)_3(H_2O)_3V_4O_{10}]^{12-}$,[6] tetrameric polyanions, $[As_4W_{40}O_{140}]^{28-}$,[7] $[Ln_3As_4W_{40}O_{140}]^{20-}$ (Ln^{III} = Ce, Nd, Sm, Gd), $[M^mLn_2As_4W_{40}O_{140}]^{(18-m)-}$ (M = Ba^{II}, K^+, none, and Ln^{III} = La, Ce, Gd),[8] $[Na_2Sb_4(H_2O)_4(SbW_9O_{33})_4]^{22-}$,[9] and $Ce_3Sb_4W_2O_8(H_2O)_{10}(SbW_9O_{33})_4^{19-}$,[10] six-meric $[(\beta\text{-}XW_9O_{33})_4(\alpha\text{-}XW_9O_{33})_2(WO_2)_4(WO(H_2O))_6WO_5(H_2O)]^{26-}$ (X = As^{3+}, Sb^{3+}),[11] and even the largest polyoxotungstate to date $[As_{12}Ce_{16}(H_2O)_{36}W_{148}O_{524}]^{76-}$ containing twelve $AsW_9O_{33}^{9-}$ building units.[12] However, the analogous vacant polyoxomolybnate Keggin anion containing the subvalent main group atoms is rather scant because of the structural lability of lacunary heteropolymolybdateas in aqueous solution. Müller and co-workers reported the existence of trivacant $\{As^{III}Mo_9O_{33}\}$ fragment in the polyanions

Received: October 26, 2011
Published: February 6, 2012

   dx.doi.org/10.1021/ic202314g | *Inorg. Chem.* 2012, 51, 2318−2324

Table 1. Summary of Crystallographic Data for the Structures of NH_4·1 and NH_4·2

	NH_4·1	NH_4·2
empirical formula	$As_2Fe_5H_{96}Mo_{21}N_{17}O_{96}$	$As_2Fe_6H_{104}Mo_{20}N_{16}O_{100}$
M, g mol^{-1}	4314.77	4332.73
cryst syst	monoclinic	monoclinic
space group	$P2_1/n$	$P2_1/n$
a (Å)	19.5756(18)	19.512(2)
b (Å)	26.105(2)	25.924(3)
c (Å)	23.470(2)	23.421(2)
V (Å^3)	11495.9(18)	11366(2)
Z	4	4
T (K)	296(2)	296(2)
d_{calcd}, g cm^{-3}	2.493	2.532
GOF	1.139	1.038
R1[a] [$I > 2\sigma(I)$]	0.0664	0.0667
wR2[b] [$I > 2\sigma(I)$]	0.1246	0.1829
R1[a] (all data)	0.1873	0.1230
wR2[b] (all data)	0.2215	0.2193
ρ_{max}, e Å^{-3}	2.214	1.954
ρ_{min}, e Å^{-3}	−1.150	−2.402

[a] $R1 = [\Sigma||F_o| - |F_c||]/[\Sigma|F_c|]$. [b] $wR2 = \{[\Sigma w(F_o^2 - F_c^2)^2]/[\Sigma w(F_o^2)^2]\}^{1/2}$.

$[(AsOH)_3(MoO_3)_3(AsMo_9O_{33})]^{7-}$, $[(AsOH)_6(MoO_3)_2(O_2Mo{-}O{-}MoO_2)_2(AsMo_9O_{33})_2]^{10-}$, and $[(AsOH)_4(AsO)_2(O_2Mo{-}O{-}MoO_2)_2(AsMo_9O_{33})_2]^{8-}$ in 1990 and 1996, respectively.[13] Recently, our group reported two new types of polyoxomolybdates based on the monocapped hexavacant α-A-Keggin subunit $As^{III}Mo_7O_{27}$ unit, namely, dimeric sandwich-like polyoxomolybdates encapsulating two transition metal ions, $[M_2(AsMo_7O_{27})_2]^{n-}$ (M = Cu^{2+}, Fe^{3+}, or Cr^{3+}) and $[FeCr(AsMo_7O_{27})_2]^{14-}$ with the antiferromagnetic exchange between the magnetic centers,[14] and double sandwich-type polyoxomolybdates encapsulating six-nuclearity clusters MFe_5, $[As_2MFe_5Mo_{22}O_{85}(H_2O)]^{n-}$ (M = Fe^{3+}, n = 14; M = Ni^{2+} and Mn^{2+}, n = 15) with the overall ferromagnetic interactions among the six-nuclearity cluster.[15] Herein, we report a novel type of double sandwich polyoxometalates, $[As_2Fe_5Mo_{21}O_{82}]^{17-}$ (**1**) and its Fe(III) substituted derivative $[As_2Fe_6Mo_{20}O_{80}(H_2O)_2]^{16-}$ (**2**), composed of a central fragment $FeMo_7O_{28}$ for **1** ($Fe_2Mo_6O_{26}(H_2O)_2$ for **2**) and two external $AsMo_7O_{27}$ fragments linked together by two distinct edge-sharing dimeric clusters Fe_2O_{10}. Both of the polyoxoanions contain a oxo-bridged Fe^{III}_5 magnetic core and the magnetism measurements show an overall ferromagnetic interactions among the five-nuclearity cluster Fe_5 with the spin ground state S = 15/2.

EXPERIMENTAL SECTION

General Methods and Materials. All chemicals were commercially purchased and used without further purification. Elemental analyses (H and N) were performed on a Perkin-Elmer 2400 CHN elemental analyzer; Fe, As, and Mo were analyzed on a IRIS Advantage ICP atomic emission spectrometer. IR spectra were recorded in the range of 400−4000 cm^{-1} on an EQUINOX55 FT/IR spectrophotometer using KBr pellets. Fluorescence spectra were measured at room temperature on a Hitachi F4500 fluorescence spectrophotometer equipped with a 450 W xenon lamp as the excitation source. UV spectra were performed on a Shimazu UV-2550 spectrophotometer. Thermogravimetry-differential scanning calorimetry (TG-DSC) analyses were performed on a NETZSCH STA 449C TGA instrument in flowing N_2 with a heating rate of 10 °C·min^{-1}. Magnetism measurements were performed on a Quantum Design MPMS SQUID magnetometer. The experimental susceptibilities were corrected for the diamagnetism of the constituent atoms (Pascal's tables).[16] MicroTOF-Q II mass spectrometer with an electrospray ionization (ESI) source (Bruker, Germany) was used. The desolvation temperature was to set to 180 °C. A capillary voltage of 2.6 kV was used in the negative scan mode, collision energy −10.0 eV. Time-of-flight mass spectra were acquired at a resolution of ∼17 500 (full width at half-maximum) at m/z 2000. Mass calibration was performed using a solution of tunemix from m/z 322 to 4000. Acetonitrile sample solutions were infused via a syringe pump directly connected to the ESI-MS source at a flow rate of 3 μL/min.

$(NH_4)_{17}[As_2Fe_5Mo_{21}O_{82}]\cdot 14H_2O$ (NH_4·1). The synthesis of compound NH_4·**1** was accomplished by adding a solution of As_2O_3 (0.08 g, 0.4 mmol) dissolved in 4 M aqueous ammonia (2 mL) to a

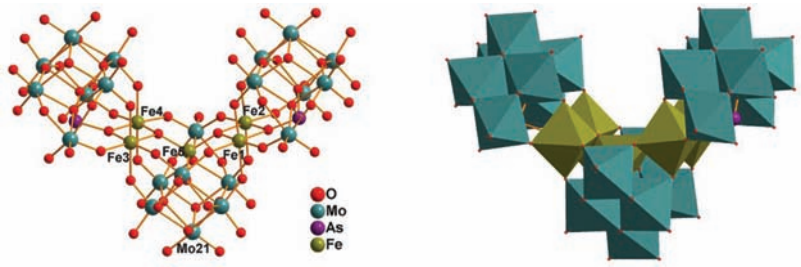

Figure 1. Ball-and-stick representation (left) and combined polyhedral representation (right) of $[As_2Fe_5Mo_{21}O_{82}]^{17-}$ (**1**).

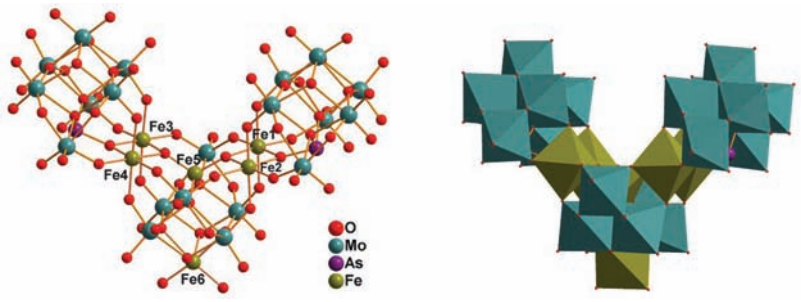

Figure 2. Ball-and-stick representation (left) and combined polyhedral representation (right) of $[As_2Fe_6Mo_{20}O_{80}(H_2O)_2]^{16-}$ (**2**).

dx.doi.org/10.1021/ic202314g | Inorg. Chem. 2012, 51, 2318−2324

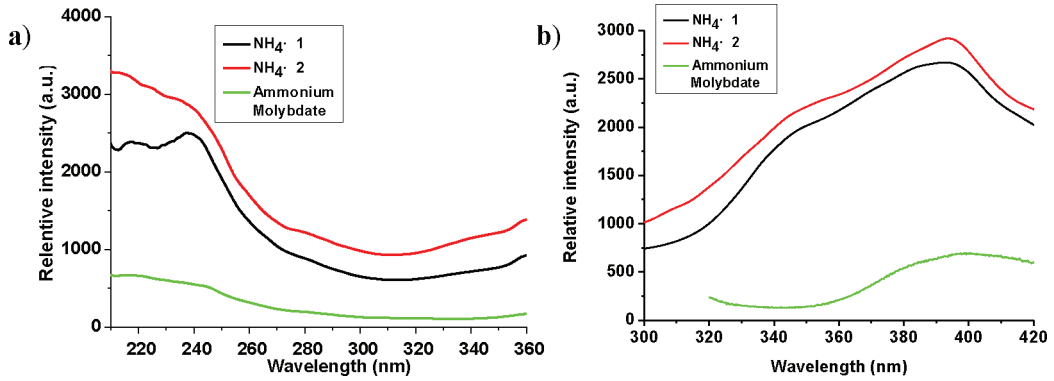

Figure 3. (a) Excitation spectra of $(NH_4)_6Mo_7O_{24}{\cdot}4H_2O$, $NH_4{\cdot}\mathbf{1}$, and $NH_4{\cdot}\mathbf{2}$ for emission at 394 nm. (**b**) Emission spectra of $(NH_4)_6Mo_7O_{24}{\cdot}4H_2O$, $NH_4{\cdot}\mathbf{1}$ and $NH_4{\cdot}\mathbf{2}$ for excitation at 240 nm. The line code is as follows: $(NH_4)_6Mo_7O_{24}{\cdot}4H_2O$ (green), $NH_4{\cdot}\mathbf{1}$ (black) and $NH_4{\cdot}\mathbf{2}$ (red).

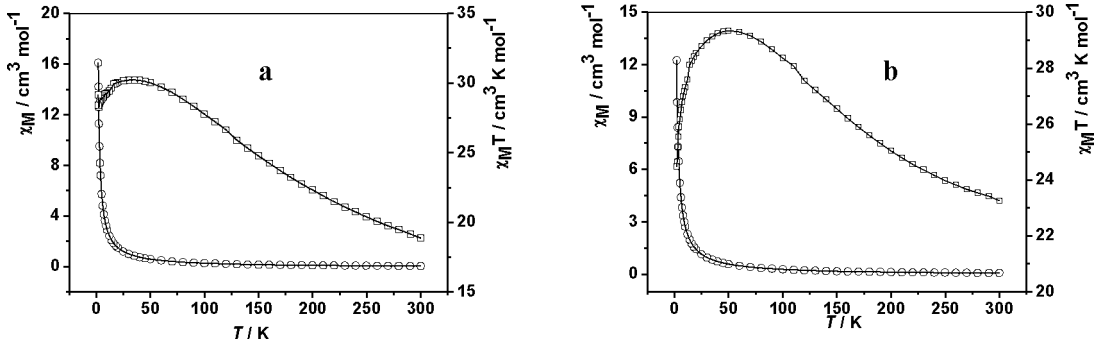

Figure 4. χ_M and $\chi_M T$ plots for polystalline samples of $NH_4{\cdot}\mathbf{1}$ (a) and $NH_4{\cdot}\mathbf{2}$ (b) at 1000 Oe applied field.

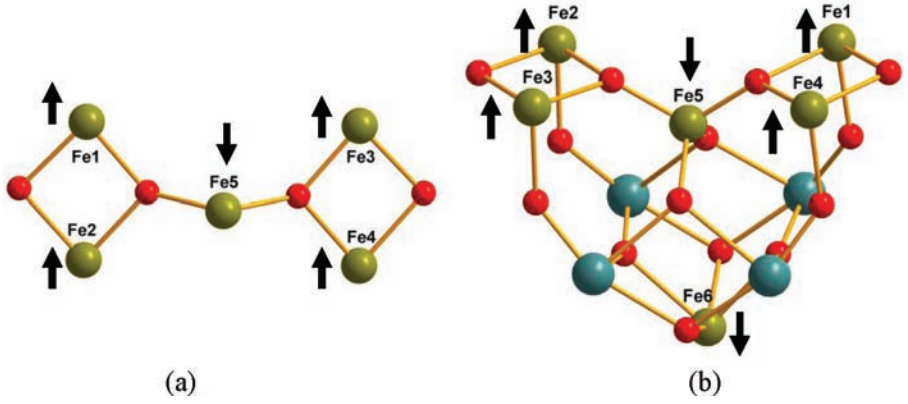

Figure 5. (a) Possible spin alignments in the Fe_5O_4 core (O, red balls; Fe, yellow-brown balls) suggesting the ground state is $S = 15/2$) for **1**. (b) Possible spin alignments in the Fe_5O_4 core and the weak antiferromagnetic between the Fe_5^{III} magnetic core and the distant Fe6 ion.

solution of $(NH_4)_6Mo_7O_{24}{\cdot}4H_2O$ (0.99 g, 0.8 mmol) dissolved in H_2O (10 mL) with vigorous stirring, and the pH was adjusted to 7.0 by adding 3 M ammonium hydroxide. Then 0.22 g (0.8 mmol) of $FeCl_3{\cdot}6H_2O$ was added to the solution. The color of the solution changed red. The reaction mixture was stirred for 60 min at 90 °C, and the mixture was allowed to cool to the ambient temperature and filtered, and the obtained solution was left to evaporate slowly at room temperature, the red block crystals were obtained after one month (yield 0.94 g, 82%, based on Mo). Elemental analysis calcd (%) for $As_2Fe_5H_{96}Mo_{21}N_{17}O_{96}$, N, 5.5; H, 2.2; Fe, 6.5; As, 3.5; Mo, 46.7. Found (%): N, 5.3; H, 2.5; Fe, 6.6; As, 3.7; Mo, 46.5. IR for $NH_4{\cdot}\mathbf{1}$(KBr, cm^{-1}): 3424(s), 3145(s), 1624(m), 918(m), 881(s), 827(m), 790(w), 677(s), 513(m) cm^{-1}.

$(NH_4)_{16}[As_2Fe_6Mo_{20}O_{80}(H_2O)_2]{\cdot}18H_2O$ ($NH_4{\cdot}\mathbf{2}$). The synthesis of $NH_4{\cdot}\mathbf{2}$ was accomplished by adding a solution of As_2O_3 (0.08 g, 0.4 mol) dissolved in 4 M aqueous ammonia (4 mL) to a solution of $(NH_4)_6Mo_7O_{24}{\cdot}4H_2O$ (0.99 g, 0.8 mmol) dissolving in (10 mL) of H_2O with vigorous stirring, the pH was adjusted to 7.0 by adding 3 M ammonium hydroxide. Then 0.22 g of $FeCl_3{\cdot}6H_2O$ (0.8 mmol) was added to the solution. The color of the solution changed red. The $H_2NCH_2CH(OH)CH_2NH_2$ (0.2 g) dissolved in H_2O (1 mL) was dropped in the solution. The reaction mixture was stirred for 60 min at 90 °C; the mixture was allowed to cool to the ambient temperature and filtered, and the obtained solution was left to evaporate slowly at room temperature, the red block crystals were obtained after one month (yield: 0.97 g, 80%, based on Mo). Elemental analysis calcd (%) for $As_2Fe_6H_{104}Mo_{20}N_{16}O_{100}$, N, 5.2; H, 2.4; Fe, 7.7; As, 3.4; Mo, 44.3. Found (%): N, 5.5; H, 2.5; Fe, 7.8; As, 3.2; Mo, 44.1. IR for $NH_4{\cdot}\mathbf{2}$ (KBr, cm^{-1}): 3421(s), 3159(s), 1621(m), 918(m), 889(m), 865(m), 825(m), 790(w), 673(s), 517(m) cm^{-1}.

dx.doi.org/10.1021/ic202314g | Inorg. Chem. 2012, 51, 2318–2324

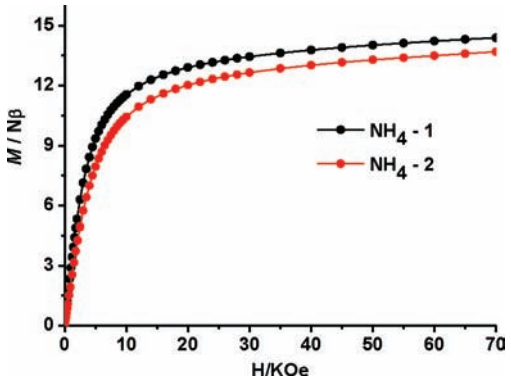

Figure 6. $M(H)$ data for polycrystalline samples of NH_4·**1** and NH_4·**2** at 2 K.

X-ray Crystallography. Intensity data were collected on a BRUKER SMART APEX II CCD diffractometer with graphite-monochromatized Mo Kα radiation (λ = 0.710730 Å) radiation at 293 (2) K. An empirical absorption correction was applied. The structures of NH_4·**1** and NH_4·**2** were solved by the direct method and refined by Full-matrix least-squares on F^2 using the SHELXTL-97 software. All heavy atoms (Mo, As, and Fe) and the framework oxygen atoms of the polyanions were refined with anisotropic displacement parameters, the other oxygen atoms were refined isotropically. Hydrogen atoms were not included but were included in the structure factor calculations. For the hydrated ammonium salt, the data did not support discrimination between oxygen and nitrogen atoms, and the ammonium ions were modeled as oxygen atoms except N1 and N2 located in special position. A summary of the crystallographic date and structure refinement for compounds NH_4·**1** and NH_4·**2** is given in Table 1.

Further details of the crystal structure investigation can be obtained from the Fachinformationszentrum Karlsruhe, 76344 Eggenstein-Leopoldshafen, Germany (fax (49)7247−808−666; e-mail crysdata@fiz-karlsruhe.de) on quoting the depository number CSD-423662 and 423663 for NH_4·**1** and NH_4·**2**, respectively.

RESULTS AND DISCUSSION

Synthesis and structure of $[As_2Fe_5Mo_{21}O_{82}]^{17-}$ and $[As_2Fe_6Mo_{20}O_{80}(H_2O)_2]^{16-}$. Polyoxometalate clusters were usually synthesized via self-assembly processes occurring in solution using routine "one-pot" syntheses. In reaction solution, there exist multiple equilibriums related to many factors such as pH, ionic strength, reaction time, temperature, counterions, concentration of starting materials and so on, and the change of any factors can affect the outcome of the reaction. The synthetic condition of NH_4·**2** is the same as that of NH_4·**1** except adding a small amount of $H_2NCH_2CH(OH)CH_2NH_2$ in the reaction process although 2-hydroxy-1,3-propylenediamine is not one of NH_4·**2**'s components, which means that the existence of 2-hydroxy-1,3-propylenediamine affects the product at the molecular level. It is worth noting that the polyoxoanions were isolated in ammonium salt. In the absence of any NH_4^+ cations, no the title compounds were obtained, which suggests that the structure is stabilized by NH_4^+ ions.

X-ray structural analysis reveals that the structure of $[As_2Fe_5Mo_{21}O_{82}]^{17-}$ exhibits C-shaped structure (Figure 1) which is composed of a central $FeMo_7O_{28}$ fragment and two external $AsMo_7O_{27}$ fragments linked together by two distinct edge-sharing dimeric clusters Fe_2O_{10}, so it can been expressed as $[(AsMo_7O_{27})(Fe_2)(FeMo_7O_{28})(Fe_2)(AsMo_7O_{27})]^{17-}$. The central $FeMo_7O_{28}$ fragment and external $AsMo_7O_{27}$ fragment have a similar structure, and both of them can be viewed as a monocapped hexavacant α-Keggin subunit with a central FeO_4 group or a central AsO_3 group. Each external $AsMo_7O_{27}$ fragment is connected with the central $FeMo_7O_{28}$ fragment in the same way, namely by two Fe^{III} ions via eight μ_2-O and two μ_3-O, to lead to a C_{2v} molecular symmetry. There are two different coordination Fe atoms in the polyanion, the Fe−O distances of the four octahedrally coordinated iron centers are in the range of 1.953(9)-2.060(10) Å and those of the tetrahedral coordinated iron in the central $FeMo_7O_{28}$ fragment are in the range of 1.821(9)−1.866(8) Å. The bond lengths and angles of the molybdenum-oxo and arsenic-oxo frameworks are within the usual ranges. The bond-valence sums (Σs) obtained from the bond strength (s) in valence units, calculated using $s = \exp[(d_0 - d)/B]$ (d_0 = 1.751, 1.789, and 1.907 Å for Fe^{3+}, As^{3+}, and Mo^{6+}, respectively, and B = 0.37 Å), are 3.03, 3.04, 3.00, and 3.11 for Fe1, Fe2, Fe3, and Fe4 in FeO_6 group, 3.12 for Fe5 in FeO_4 group, respectively; 3.03 and 2.88 for As1 and As2; average 6.05 for Mo atoms, which suggests that the valency of all the atoms remains unchanged.

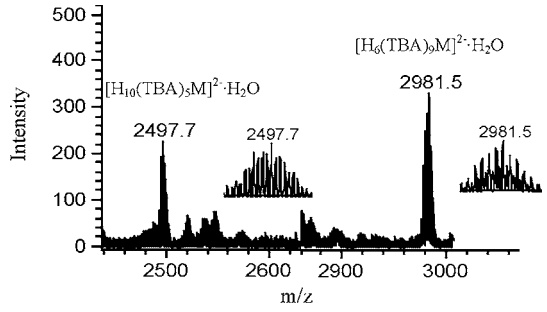

Figure 7. Negative ESI-MS spectrum of CH_3CN:H_2O = 1:1 solutions of NH_4·**1** in the range from m/z 2420 to 3010.

The monocapped molybdenum atom in the central $FeMo_7O_{28}$ fragment of **1** can be replaced by a Fe^{III} ion to form isostructural $[As_2Fe_6Mo_{20}O_{80}(H_2O)_2]^{16-}$ (**2**) with two terminal water (Figure 2). The bond-valence sums (Σs) obtained from the bond strength (s) in valence units are 3.07, 3.09, 3.03, 3.02, and 3.00 for Fe1, Fe2, Fe3, Fe4, and Fe6 in FeO_6 group, 4.13 for Fe5 in FeO_4 group, respectively; 3.04 and 3.01 for As1 and As2; average 6.11 for Mo atoms. The abnormally high BVS value of 4 for Fe5 may be due to the existence of strong polarization around FeO_4 group in the compound. It is interesting that both of polyoxoanions **1** and **2** contain a oxo-bridged Fe^{III}_5 magnetic core with the angles of Fe−O−Fe in the range of 96.4(4)−125.7(5)°, so their interesting magnetic properties can be expected. It should be mentioned that two plausible nitrogen atoms could be discriminated both in NH_4·**1** and in NH_4·**2**, ammonium cations (N1 and N2) are wrapped in the C-shaped structure by strong hydrogen bonds with the distance of N···O and N···N in the range of 2.71−3.00 Å (Supporting Information Figure S1).

The structure of the polyanions represents a new type of double sandwich POM, which is different from that of the reported C-shaped polyoxotungstates, such as $[Ni_6As_3W_{24}O_{94}(H_2O)_2]^{17-}$, $[Ni_4Mn_2P_3W_{24}O_{94}(H_2O)_2]^{17-}$,[17] $[(MOH_2)M_2PW_9O_{34})_2(PW_9O_{26})]^{17-}$ (M = Co^{2+}, Mn^{2+}),[18] $[Mn_6Ge_3W_{24}O_{94}(H_2O)_2]^{18-}$,[19] $[M_6Ge_3W_{24}O_{94}(H_2O)_2]^{n-}$ (M = Fe^{III}, n = 14; M = Co^{II}, n = 20; M = Mn^{II}/Mn^{III}, n = 18),[20] $\{Co(Hen)-[Co_6As_3W_{24}O_{94}(H_2O)_2]\}_2^{28-}$,[21] and $[(Fe_4W_9O_{34}(H_2O)_2)_2(FeW_6O_{26})]^{19-}$,[22] all of them consist of two trivacant Keggin moieties XW_9O_{34} and a central XW_6O_{26} fragment linked via two M_3 cluster leading to a banana-shaped structure with C_{2v} symmetry. It is also different from that of the reported C-shaped polyoxomolybdates, $[As_2Fe_5MMo_{22}O_{85}(H_2O)]^{n-}$ (M = Fe^{3+}, n = 14; M = Ni^{2+} and Mn^{2+}, n = 15),[17] consists of a central

dx.doi.org/10.1021/ic202314g | Inorg. Chem. 2012, 51, 2318−2324

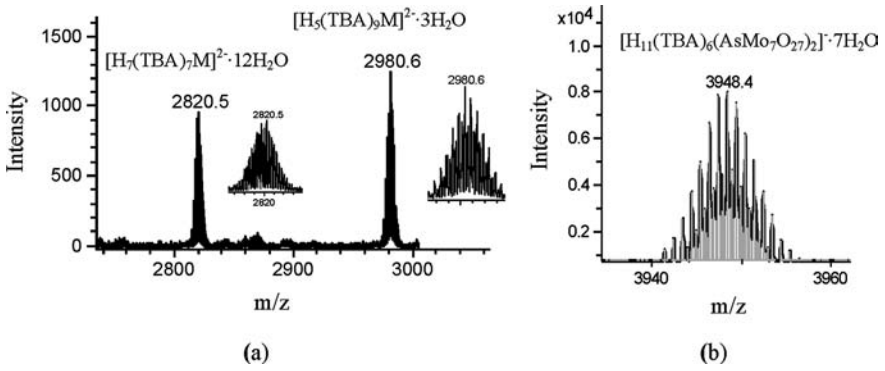

Figure 8. (a) Negative ESI-MS spectrum of CH_3CN:H_2O = 1:1 solutions of NH_4·**2** in the range from m/z 2420 to 3010. (b) the peak from $[H_{11}(TBA)_6(AsMo_7O_{27})_2]^-$·$7H_2O$ (m/z = 3948.4).

MMo_7O_{28} fragment and two $AsMo_7O_{27}$ fragments liked together by two trimeric clusters, $Fe_2MoO(\mu_2\text{-}o)_2$ and $Fe_3(H_2O)$, to form a banana-shaped structure with C_1 symmetry.

FT-IR Spectra. IR spectra of NH_4·**1** and NH_4·**2** are similar. Take NH_4·**1** as an example, the strong band at 918 cm^{-1} can be assigned to the characteristic vibration of υ(Mo−O_d), the bands at 881 and 827 cm^{-1} to those of υ(Mo−O_d−Mo) or As−O, the bands at 790 and 677 cm^{-1} to υ(Mo−O_c−Mo). The bands at 3421 and 1621 cm^{-1} are ascribed to water molecules, respectively. The band at 3159 cm^{-1} ascribed to the N−H stretching vibration of ammonium ion. The main difference between NH_4·**1** and NH_4·**2** is that the band at 881 cm^{-1} for NH_4·**1** is split to two bands at 889(m) and 865(m) cm^{-1} for NH_4·**2**.

Fluorescent Spectroscopy. The photoluminescent properties of $(NH_4)_6Mo_7O_{24}$·$4H_2O$, NH_4·**1**, and NH_4·**2** were investigated in the solid state at room temperature (Figure 3). For excitation spectra (Figure 3a), all of three compounds, $(NH_4)_6Mo_7O_{24}$·$4H_2O$, NH_4·**1**, and NH_4·**2**, exhibit an absorbance maxima at ∼240 nm for emission at 394 nm. For emission spectra (Figure 3b), $(NH_4)_6Mo_7O_{24}$·$4H_2O$ presents a weak broad fluorescence emission band with the maximum value at ∼398 nm in the solid state upon excitation at 240 nm, which corresponds to O−Mo charge transfer. The emission bands of NH_4·**1** and NH_4·**2** are compared to that of ammonium molybdate and both exhibit an intense emissions at λ_{max} = 394 nm and a broad shoulder at 347 nm.

Thermal Analyses. According to the TG-DSC curve of compound NH_4·**1** (Figure S3a, Supporting Information), we can deduce that the thermal decomposition process of the compound is approximately divided into three steps. First, it gradually loses all water and NH_3 molecules in the range 30−325 °C, and a weight loss of 12.0% is comparable with the calculated value of 12.6%. The second weight loss of 4.7%(calcd 4.6%) is between 310 to 400 °C, accompanying an exothermal peak at 330 °C in the DSC curve due to the escaping of As_2O_3. The third stage is the decomposition of the Mo−Fe−O framework structure accompanying an exothermal peak at 456 °C in the DSC cure. The final product should be the mixed metal oxide 2.5 Fe_2O_3 + 21MoO_3, and the observed total weight loss of 20.9% compares well with the calculated value of 20.7%. For NH_4·**2**, the thermal decomposition process of compound NH_4·**2** (Figure S3b, Supporting Information) is similar with that of compound NH_4·**1**. It gradually loses all water and NH_3 in the range of 30−325 °C, and a weight loss of 13.9% is comparable with the caculated value of 14.6%. The second weight loss of 4.1% (calcd 4.6%) is between 325 to 409 °C because of the escaping of As_2O_3. The final product should be the mixed metal oxide 3Fe_2O_3 + 20MoO_3, and the observed total weight loss of 23.1% compares with the calculated value of 22.5%.

Magnetic Properties. The magnetic properties of compounds NH_4·**1** and NH_4·**2** were measured with an applied field of H = 1000 Oe in the temperature range 2.0−300.0 K. Figure 4a shows the $\chi_M T$ and χ_M plots of NH_4·**1**, the $\chi_M T$ product at room temperature is 18.88 cm^3 mol^{-1} K, is slightly lower than the expected spin-only value of 21.87 cm^3 mol^{-1} K for five uncoupled Fe^{III} centers (S = 5/2, g = 2.00 for each Fe^{III} ion). When the temperature is lowered, the $\chi_M T$ product increases from ambient temperature down to 35 K with a maximum of 30.22 cm^3 mol^{-1} K, then decreasing slowly to 28.4 cm^3 K mol^{-1} at 2 K. This behavior demonstrates that the ferromagnetic and antiferromagnetic interactions coexist in the Fe_5 magnetic centers. The value of 30.22 cm^3 mol^{-1} K can be compared with the expected value of 31.87 cm^3 mol^{-1} K (g_{Fe} = 2, S_{Fe} = 15/2) for the five spin-couple Fe^{III} ions with S = 15/2 spin ground state, deducing from magnetostructural correlations,[23] namely, antiferromagnetic coupling between the tetrahedral coordinated Fe^{III} and octahedrally coordinated Fe^{III} centers through one μ-oxo group with the angles of Fe_{tetra}−O−Fe_{octa} in the range of 123.9(4)−125.0(4)°, and ferromagnetic coupling between octahedrally coordinated Fe^{III} centers of dimeric clusters Fe_2O_{10} with the angles in the range of 96.4(4)−100.4(4)° (Figure 5a). The drop in the $\chi_M T$ value below the apex temperature suggests the presence of significant zero-field splitting (ZFS) effects in the ground state or molecular interactions. According to the previous structure analysis, the data were simulated considering two different coupling constants J_1 and J_2 using the spin Hamiltonian below in eq 1:

$$\hat{H} = -2J_1(\hat{S}_1\hat{S}_5 + \hat{S}_2\hat{S}_5 + \hat{S}_3\hat{S}_5 + \hat{S}_4\hat{S}_5) - 2J_2(\hat{S}_1\hat{S}_2 + \hat{S}_3\hat{S}_4) \quad (1)$$

An intercluster interaction θ was also included as a mean field correction. The best fit leads to the following parameters: g = 2.02, J_1 = −16.2 cm^{-1}, J_2 = 23.4 cm^{-1}, and θ = −1.0 K. The J_1 and J_2 values confirm that appreciably different magnetic interaction are mediated through the μ-oxo group with the different Fe−O−Fe angles.

The magnetic behavior of NH_4·**2** could be expected to be analogous to NH_4·**1** owing to their isostructural, and only difference is that the monocapped molybdenum atom in the central $FeMo_7O_{28}$ fragment of **1** is substituted by a Fe^{III} ion, spaced four chemical bonds from other Fe^{III} ion of Fe^{III}_5 magnetic core. The temperature dependence of χ_M and $\chi_M T$ product of NH_4·**2** is shown in Figure 4b. At room temperature, the value

dx.doi.org/10.1021/ic202314g | Inorg. Chem. 2012, 51, 2318−2324

of $\chi_M T$ per $[As_2Fe_6Mo_{20}O_{80}(H_2O)_2]^{16-}$ unit is 23.35 cm^3 mol^{-1} K and is slightly lower than the expected value of 26.25 cm^3 mol^{-1} K for the six isolated Fe^{III} ions ($S = 5/2$, $g = 2.00$). The $\chi_M T$ product increases continually on lowering the temperature from 300 to 45 K, and reaches a maximum value of 29.45 cm^3 mol^{-1} K at 45 K, then decreasing to 6 emu K mol^{-1} at 2 K. The maximum value of 29.45 cm^3 mol^{-1} K for NH_4·**2** is little lower than that of 30.22 cm^3 mol^{-1} K for NH_4·**1**, which means that the weak antiferromagnetic interactions between the Fe^{III}_5 magnetic core (31.87 cm^3 mol^{-1} K, $g_{Fe} = 2$, $S_T = 15/2$) and the distant Fe6 ion (Figure 5b). According to the magnetic structure analysis, the data were simulated using the equation:

$$\chi_{Fe_6} = \chi_{Fe_5} + \frac{Ng^2\beta^2}{3kT} S_{Fe}(S_{Fe} + 1)$$

θ was also included as a mean field correction as well as the interaction between Fe_5 center and the substituted Fe6 ion. The best fit gives g = 2.04, $J_1 = -9.8$ cm^{-1}, $J_2 = 24.0$ cm^{-1}, and $\theta = -0.45$ K.

As shown in Figure 6, the M values for NH_4·**1** increase with increasing magnetic field and reach a value of 14.45 Nβ at 70 KOe and 2 K, which is also good agreement with an $S = 15/2$ spin ground state. For NH_4·**2**, the M values increase with increasing magnetic field and reach a value of 13.79 Nβ at 70 KOe, which is slightly lower than an $S = 15/2$ spin ground state for NH_4·**1**, further demenstrating the weak antiferromagnetic coupling between the Fe^{III}_5 magnetic core and the distant Fe^{III} center.

UV Spectra. The stability of the polyanions **1** and **2** in water has been studied using the time-dependent UV spectra of a 0.01 mM aqueous solution (pH = 6.5). For NH_4·**1** (Supporting Information Figure S4a), two absorption bands at 207 nm and 229 can be assigned to the $O_d \rightarrow$ Mo and $O_b/O_c \rightarrow$Mo charge transfer transition, respectively. In the case of NH_4·**2** (Supporting Information Figure S4b), only one absorption band located at $\lambda_{max} = 215$ nm is observed and assigned to the O → Mo charge transfer transition. With the extension of time, the maximum absorption intensity at ~210 nm decreases, which may mean that part of the polyanions dissociate in the aqueous solution.

Electrospray Mass Spectra. The negative mode electrospray mass spectra of NH_4·**1** and NH_4·**2** dissolved in CH_3CN/H_2O = 1:1 solution and in the presence of $(C_4H_9)_4NBr$ are shown in Figures 7 and 8, respectively. For NH_4·**1**, the two peaks centered at m/z = 2497.7 and 2981.5, regularly spaced with $\Delta m/z = 0.5$ which imply a 2− charge are observed and could be assigned to $[H_{10}(TBA)_5\cdot\mathbf{1}]^{2-}\cdot H_2O$ and $[H_6(TBA)_9\cdot\mathbf{1}]^{2-}\cdot H_2O$ (TBA = $(C_4H_9)_4N^+$), respectively. For NH_4·**2**, the two peaks located at m/z = 2820.5, 2980.6, regularly spaced with $\Delta m/z = 0.5$ which imply a 2− charge could be attributed to $[H_5(TBA)_9\cdot\mathbf{2}]^{2-}\cdot 3H_2O$ and $[H_7(TBA)_7\cdot\mathbf{2}]^{2-}\cdot 12H_2O$. The results show that the intact polyanions **1** and **2** exist in solution. In addition, a peak from $[H_{11}(TBA)_6(AsMo_7O_{27})_2]^-\cdot 7H_2O$ (m/z = 3948.4) of dimeric $AsMo_7O_{27}$ moiety is also observed (Figure 8b), which provide further proof that the fragment $AsMo_7O_{27}$ is a basic building unit to construct large polyoxomolybdates.

CONCLUSIONS

In conclusion, we have selectively synthesized a novel type of double sandwich polyoxometalates, $[As_2Fe_5Mo_{21}O_{82}]^{17-}$ and its Fe(III) substituted derivative $[As_2Fe_6Mo_{20}O_{80}(H_2O)_2]^{16-}$, by adding a small amount 2-hydroxy-1,3-propylenediamine in the reaction process. Both of the double sandwich polyoxometalates contain a oxo-bridged Fe^{III}_5 magnetic core and magnetism measurements show an overall ferromagnetic interactions among center five-nuclearity clusters Fe_5 with the spin ground state $S = 15/2$. The successful synthesis of the new type polyoxometalates based on $AsMo_7O_{27}$ fragment and the observation of the fragment $AsMo_7O_{27}$ by electrospray ionization mass spectrometry (ESI-MS) studies of the title polyoxometalates dissolved in acetonitrile solution further prove that the $AsMo_7O_{27}$ is a basic building unit to construct large polyoxomolybdates.

ASSOCIATED CONTENT

Supporting Information

FT-IR spectra, UV spectra, TG-DSC curves, crystallographic data in CIF format for compounds NH_4·**1** and NH_4·**2**, and χ derivation for the Fe^{III}_5 magnetic core. This material is available free of charge via the Internet at http://pubs.acs.org.

AUTHOR INFORMATION

Corresponding Author

*E-mail: xglin707@163.com.

ACKNOWLEDGMENTS

This research was supported by National Natural Science Foundation of China (20973133), the Natural Science Foundation of Shaanxi Province (2009JQ7010) and the Education Commission of Shaanxi Province (09JK761 and 09JK783).

REFERENCES

(1) (a) Pope, M. T. *Heteropoly and Isopoly Oxometalates*; Springer-Verlag: Berlin, Germany, 1983. (b) Pope, M. T.; Müller, A. *Polyoxometalate Chemistry: From Topology via Self-Assembly to Applications*; Kluwer: Dordrecht, The Netherlands, 2001. (c) Pope, M. T.; Yamase, T. *Polyoxometalate Chemistry for Nanocomposite Design*; Kluwer: Dordrecht, The Netherlands, 2002. (d) Borràs-Almenar, J. J., Coronado, E., Müller, A., Pope, M. T., Eds. *Polyoxometalate Molecular Science*; Kluwer: Dordrecht, the Netherlands, 2003. (e) Pope, M. T. *In Comprehensive Coordination Chemistry II*; McCleverty, J. A., Meyer, T. J., Eds.; Elsevier Ltd.: Oxford, U.K., 2004. (f) Long, D.-L.; Burkholder, E.; Cronin, L. *Chem. Soc. Rev.* **2007**, *36*, 105. (g) Kortz, U.; Müller, A.; van Slageren, J.; Schnack, J.; Dalal, N. S.; Dressel, M. *Coord. Chem. Rev.* **2009**, *253*, 2315.

(2) (a) Nishiyama, Y.; Nakagawa, Y.; Mizuno, N. *Angew. Chem., Int. Ed.* **2001**, *40*, 3639. (b) Botar, B.; Geletii, Y. V.; Kögerler, P.; Musaev, D. G.; Morokuma, K.; Weinstock, I. A.; Hill, C. L. *J. Am. Chem. Soc.* **2006**, *128*, 11268. (c) Brockman, J. T.; Stamatatos, T. C.; Wernsdorfer, W.; Abboud, K. A.; Christou, G. *Inorg. Chem.* **2007**, *46*, 9160. (d) Stamatatos, T. C.; Abboud, K. A.; Wernsdorfer, W.; Christou, G. *Angew. Chem., Int. Ed.* **2007**, *46*, 884.

(3) (a) Bösing, M.; Loose, I.; Pohlmann, H. *Chem.—Eur. J.* **1997**, *3*, 1232. (b) Loose, I.; Droste, E.; Bösing, M.; Pohlmann, H.; Dickman, M. H.; Rosu, C.; Pope, M. T.; Krebs, B. *Inorg. Chem.* **1999**, *38*, 2688. (c) Kortz, U.; Al-Kassem, N. K.; Savelieff, M. G.; Al Kadi, N. A.; Sadakane, M. *Inorg. Chem.* **2001**, *40*, 4742. (d) Mialane, P.; Marrot, J.; Rivière, E.; Nebout, J.; Hervé, G. *Inorg. Chem.* **2001**, *40*, 44. (e) Kortz, U.; Savelieff, M. G.; Bassil, B. S.; Keita, B.; Nadjo, L. *Inorg. Chem.* **2002**, *41*, 783. (f) Volkmer, D.; Bredenkötter, B.; Tellenbröker, J.; Kögerler, P.; Kurth, D. G.; Lehmann, P.; Schnablegger, H.; Schwahn, D.; Piepenbrink, M.; Krebs, B. *J. Am. Chem. Soc.* **2002**, *124*, 10489. (g) Bi, L.-H.; Reicke, M.; Kortz, U.; Keita, B.; Nadjo, L.; Clark, R. J. *Inorg. Chem.* **2004**, *43*, 3915. (h) Liu, H.; Qin, C.; Wei, Y.-G.; Xu, L.; Gao, G.-G.; Li, F.-Y.; Qu, X.-S. *Inorg. Chem.* **2008**, *47*, 4166. (i) Kortz, U.; Müller, A.; van Slageren, J.; Schnack, J.; Dalal, N. S.; Dressel, M. *Coord. Chem. Rev.* **2009**, *253*, 2315.

(4) Hussain, F.; Kortz, U.; Clark, R. J. *Inorg. Chem.* **2004**, *43*, 3237.

(5) Ibrahim, M.; Mal, S. S.; Bassil, B. S.; Banerjee, A.; Kortz, U. *Inorg. Chem.* **2011**, *50*, 956.

(6) Botar, B.; Yamase, T.; Ishikawa, E. *Inorg. Chem. Commun.* **2000**, *3*, 579.
(7) Robert, F.; Leyrie, M.; Hervé, G.; Tézé, A.; Jeannin, Y. *Inorg. Chem.* **1980**, *19*, 1746.
(8) Wassermann, K.; Pope, M. T. *Inorg. Chem.* **2001**, *40*, 2763.
(9) Bösing, M.; Loose, I.; Pohlmann, H.; Krebs, B. *Chem.—Eur. J.* **1997**, *3*, 1232.
(10) Xue, G.; Vaissermann, J.; Gouzerh, P. *J. Clust. Sci.* **2002**, *13*, 409.
(11) Kortz, U.; Savelieff, M. G.; Bassil, B. S.; Dickman, M. H. *Angew. Chem., Int. Ed.* **2001**, *40*, 3384.
(12) Wassermann, K.; Dickman, M. H.; Pope, M. T. *Angew. Chem., Int. Ed. Engl.* **1997**, *36*, 1445.
(13) (a) Müller, A.; Krickemeyer, E.; Penk, M.; Wittenben, V.; Döring, J. *Angew. Chem., Int. Ed. Engl.* **1990**, *29*, 88. (b) Müller, A.; Krickemeyer, E.; Dillinger, S.; Meyer, J.; Bögge, H.; Stammlar, A. *Angew. Chem., Int. Ed. Engl.* **1996**, *35*, 171.
(14) (a) Li, L.; Shen, Q.; Xue, G.; Xu, H.; Hu, H.; Fu, F.; Wang, J. *Dalton Trans.* **2008**, 5698. (b) Xu, H.; Li, L.; Liu, B.; Xue, G.; Hu, H.; Fu, F.; Wang, J. *Inorg. Chem.* **2009**, *48*, 10275.
(15) Liu, B.; Li, L.; Zhang, Y.; Ma, Y.; Hu, H.; Xue, G. *Inorg. Chem.* **2011**, *50*, 9172.
(16) Kahn, O. *Molecular Magnetism*; VCH Publisher: New York, 1993.
(17) Mbomekalle, I. M.; Keita, B.; Nierlich, M.; Kortz, U.; Berther, P.; Nadijo, L. *Inorg. Chem.* **2003**, *42*, 5143.
(18) Ritorto, M. D.; Anderson, T. M.; Nieiwert, W.; Hill, C. L. *Inorg. Chem.* **2004**, *43*, 44.
(19) Jing, N.; Li, F.; Xu, L.; li, Y.; Li, J. *Inorg. Chem. Commun.* **2010**, *13*, 372.
(20) (a) Keisuke, F.; Toshihiro, Y. *Bull. Chem. Soc. Jpn.* **2007**, *80*, 178. (b) Li, B.; Zhao, J.; Zheng, S.; Yang, G. *Inorg. Chem. Chem.* **2009**, *12*, 69. (c) Tong, R. Z.; Chen, L. L.; Liu, B.; Xue, G. L.; Hu, H. M.; Fu, F.; Wang, J. W. *Inorg. Chem. Commun.* **2010**, *13*, 98.
(21) Ma, P.; Chen, L.; Zhao, J.; Wang, W.; Wang, J.; Niu, J. *Inorg. Chem. Commun.* **2011**, *14*, 415.
(22) Compain, J.-D.; Mialane, P.; Dolbecq.; Mbomekalle, I. M.; Marrot, J.; Sécheresse, F.; Rivière, E.; Rogez, G.; Wernsdorfer, W. *Angew. Chem., Int. Ed.* **2009**, *48*, 3077.
(23) Canana-Vilalta, C.; O'Brien, T. A.; Brechin, E. K.; Pink, M.; Davidson, E. R.; Christou, G. *Inorg. Chem.* **2004**, *43*, 5505.